Palaeogeography, Palaeoclimatology, Palaeoecology 534 (2019) 109289

Contents lists available at ScienceDirect

Palaeogeography, Palaeoclimatology, Palaeoecology

journal homepage: www.elsevier.com/locate/palaeo

The effect of seasonal rainfall on nutrient input and biological productivity in the Yax Chen cave system (Ox Bel Ha), Mexico, and implications for μXRF core studies of paleohydrology

Chelsi A. McNeill-Jewer[a,*], Eduard G. Reinhardt[a], Shawn Collins[a,b], Shawn Kovacs[a,c], Winnie May Chan[a,d], Fred Devos[e], Chris LeMaillot[e]

[a] McMaster University, School of Geography and Earth Sciences, Hamilton, ON L8S 4K1, Canada
[b] Wireline Services Group, Unit 28 – 80 Barbados Blvd., Toronto, ON M1J 1K9, Canada
[c] GEM Systems Inc., 135 Spy Court, Markham, ON L3R 5H6, Canada
[d] CNRS - Université de Lyon 2, UMR 5133, Archéorient de Maison de l'Orient et de la Méditerranée, 7 Rue Raulin 69007, Lyon, France
[e] Mexico Cave Exploration Project (MCEP), Centro Investigador del Sistema Acuifero de Quintana Roo A.C. (CINDAQ), Global Underwater Explorers (GUE), Mexico

ARTICLE INFO

Keywords:
Sediment traps
Weathering proxies
Yucatan Peninsula
Anchialine caves
μXRF core scanning
Hurricanes
Mangrove

ABSTRACT

Lakes and speleothems from Mexico's Yucatan Peninsula have been used extensively over the past decades for paleoclimate studies, however aquifer condition and its response to climate change has received little attention. Cenotes (sinkholes) and coastal caves have been shown to record the paleohydrology of the aquifer, but there is little information on sedimentation in these cave systems and its response to climate change. Newly developed μXRF instrumentation for the analysis of cores can achieve subannual resolution due to small measurement increments, but short period studies examining weathering inputs and rainfall have not yet been undertaken, hindering paleoenvironmental interpretations of lake and cave sediment records. This study examines the spatial and temporal relationship of cave sediment geochemistry in the anchialine cave system of Yax Chen (Quintana Roo, Mexico). Sediment traps (n = 51) were placed at seventeen stations along the 2.7 km flooded cave system, which transitions from mangrove to upland forest terrain, with cenotes of variable size and frequency along its length. Sediment traps were collected every ~6 months from May 2013–May 2017 along with rainfall and groundwater level data. There are distinct responses of lithogenic (Fe, Ti, Sr - limestone weathering) and biogenic influenced (Si, K, S - phytoplankton and mangrove sediment) elements in the sediment samples associated with seasonal rainfall and hurricanes. While lithogenic elements (Ti/K) show a direct relationship seasonal rainfall, the sedimentation of biologically influenced (Si/Ti) elements exhibit a 6–12 month lagged response with large rainfalls such as Hurricane Ingrid in 2013 and other tropical storms throughout the study period.

1. Introduction

Weathering proxies are commonly used for paleoenvironmental analysis of lake and ocean sediments and often include measurements of potassium (K), iron (Fe) and titanium (Ti) (Haug et al., 2001; Kylander et al., 2011). Recent instrumental advances have now allowed these elements to be measured at high resolution with more efficiency using automated μXRF core scanners. Earlier studies used bulk sediment analyses (e.g. ICP-MS, XRF, etc.) of these elements and others (e.g. Ca and Sr) to understand changing weathering inputs and relationships with climate change (e.g. wet/dry), but these studies are of relatively low resolution and thus only document large trends (Zhao and Zheng, 2015). A significant amount of research has been devoted to understanding rock weathering rates over geological timescales due to its importance in carbon cycling. Climate change and sediment core studies often rely on this body of research to make inferences on changing environmental conditions (Gaillardet et al., 2018; Lo et al., 2017). The recent advent of μXRF core scanners has allowed an increased number of high-resolution weathering records that reveal smaller, annual to sub-annual trends in periodicity (e.g., Orme et al., 2016), however there is a lack of data to assess the sensitivity of these proxies to seasonal or spatial trends on a basin level.

In order to estimate the sensitivity of weathering proxies to seasonal changes, one can use previous studies such as those examining

* Corresponding author.
E-mail addresses: mcneic3@mcmaster.ca (C.A. McNeill-Jewer), shawncollins@wirelineservices.com.au (S. Collins), shawn.kovacs@gemsystems.ca (S. Kovacs), fred@zerogravity.com.mx (F. Devos), chris@zerogravity.com.mx (C. LeMaillot).

https://doi.org/10.1016/j.palaeo.2019.109289
Received 8 March 2019; Received in revised form 12 July 2019; Accepted 23 July 2019
Available online 26 July 2019

dissolved and suspended sediment loads of rivers and streams and spatial patterning of surface sediments from lake or ocean basins (Dauvalter and Rognerud, 2001; Froger et al., 2018). However, such studies may not be applicable as they may not include elements of interest, or record the necessary weather patterns (e.g. rainfall) and the catchment geology may be quite different. Further complications arise when comparing data that uses different analytical methods (XRF, ICPMS, etc.) and sampling strategies (i.e. dissolved and suspended load, surface sediment samples; Gregory et al., 2019). μXRF core scanning measures bulk sediment including porewater and sediment, which limits comparisons with this previous data (e.g. Gregory et al., 2019). Spatial surface samples within the basin and along environmental gradients of interest (eg. proximity to fluvial input) can be used, but surface samples have variable time averaging and thus have limitations when examining short-term seasonal or weather-related trends (Gregory et al., 2017; Roy et al., 2018). Sediment trap studies are more useful in this regard, but as sediment traps are more logistically intensive in terms of deployment and recovery, there are only a few studies to draw upon (Urban et al., 2004; Bischoff et al., 2005; Collins et al., 2015a)

Here we present four years of μXRF elemental data from sediment traps analyzed using the Sequential Sample Reservoir (SSR), which can be directly compared with μXRF core records (Gregory et al., 2017). Sediment trap samples were collected every ~ 6 months from Yax Chen, which is part of the Ox Bel Ha cave system in the Yucatan Peninsula, Mexico. Yax Chen is the location of an ongoing environmental monitoring project beginning in 2011 to document aquifer hydrology and sedimentation (Collins et al., 2015a, 2015b; Coutino et al., 2017; Kovacs et al., 2017). This data is important as it provides baseline information on the sensitivity and response of weathering and productivity proxies (Fe, Ti, K, Si) for paleohydrological assessment of cave sediment records (μXRF) on which there is little prior research, but also provides insight for other paleolimnological studies in karst terrains (Roy et al., 2018).

2. Site background

2.1. Yucatan Karst

The Yucatan Peninsula (Fig. 1) is a Cretaceous-Cenozoic karstified limestone platform over 350,000 km^2 in area located in southeast Mexico, bordered by the Gulf of Mexico and the Caribbean Sea (Smart et al., 2006). The coastal Quaternary deposits are relatively flat, resulting in a low hydraulic gradient (10–15 cm/km) and flow towards the coast (Beddows, 2004). The limestone has a high net porosity ranging from 14 to 23% that is both vertically and horizontally anisotropic, and groundwater flow occurs through matrix porosity, fractures, and cave conduits, with the majority of flow (~99%) within the conduits (Beddows, 2004; Beddows et al., 2007; Smart et al., 2006). The high porosity focuses percolation of rainwater to the subsurface rather than ponding on the surface, resulting in a relative scarcity of surficial lakes and rivers in the region. Multiple phases of dissolution associated with sea-level change have created extensive wet and dry cave conduits, sinkholes/karst windows (locally known as cenotes), and submarine vents that discharge meteoric water at points along the coast (Back and Hanshaw, 1970, Beddows, 2004; Paytan et al., 2006; Smart et al., 2006). The conduits are generally aligned perpendicular to the coast and cause increased turbulent flow and transmissivity within the groundwater mass (Beddows, 2004; Bauer-Gottwein et al., 2011). The morphology of the conduits is important controls on the distribution of groundwater throughout the region (Beddows, 2004; Smart et al., 2006). Though the majority of caves do not have substantial sediment accumulation, depending on vegetation coverage and sinkhole size, some passages downstream of cenotes contain allochthonous organic material from the open water where primary productivity occurs (Pohlman et al., 1997; Sánchez et al., 2002; Smith et al., 2002; Collins et al., 2015a). Compared to other regions of Mexico, the chemical composition of sedimentary archives from the Yucatan Peninsula has received little attention (Curtis et al., 1996; Hodell et al., 2005; Carrillo-Bastos et al., 2010), though there are many studies that focus on other methods of paleoecological reconstruction.

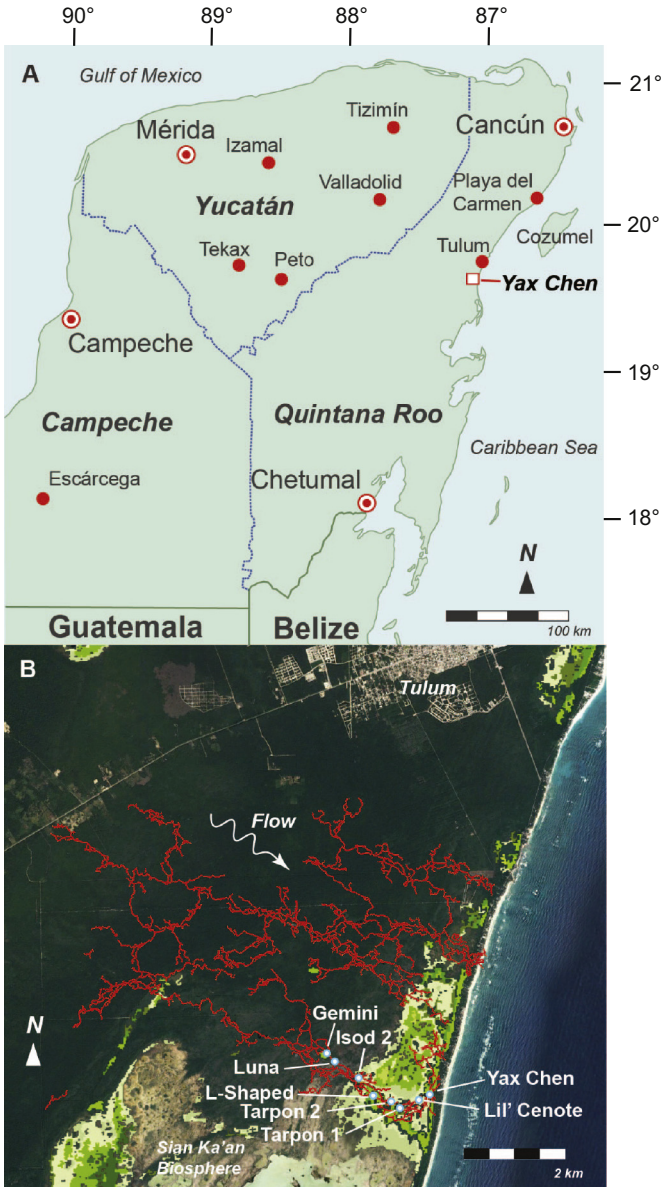

Fig. 1. A) Map of the Yucatan Peninsula showing location of Yax Chen Cave System. B) Map of the Ox Bel Ha Cave System (red lines) which at present has ~270 km of mapped passage (QRSS, 2019). Yax Chen is a 2.7 km NW-SE trending section of Ox Bel Ha to the north of the Sian Ka'an Biosphere Reserve. Shown are the cenotes as in Fig. 2 with the classified mangrove type of fringe and dwarf mangrove (dark and light green; see Collins et al., 2015a for full description). (For interpretation of the references to colour in this figure legend, the reader is referred to the web version of this article.)

2.2. Yucatan aquifer and Yax Chen hydrology

Within the Yucatan subsurface, the Meteoric or fresh Water Mass (MeWM) (< 1 ppt) is stratified overtop a denser Marine Water Mass (MaWM) (> 30 ppt). The two water masses are separated by a boundary of intermediate salinity (halocline/picnocline) that responds to wet/dry cycles, sea-level rise, tidal mixing and storms. Response to storms has recently been documented by salinity sensors within the Ox

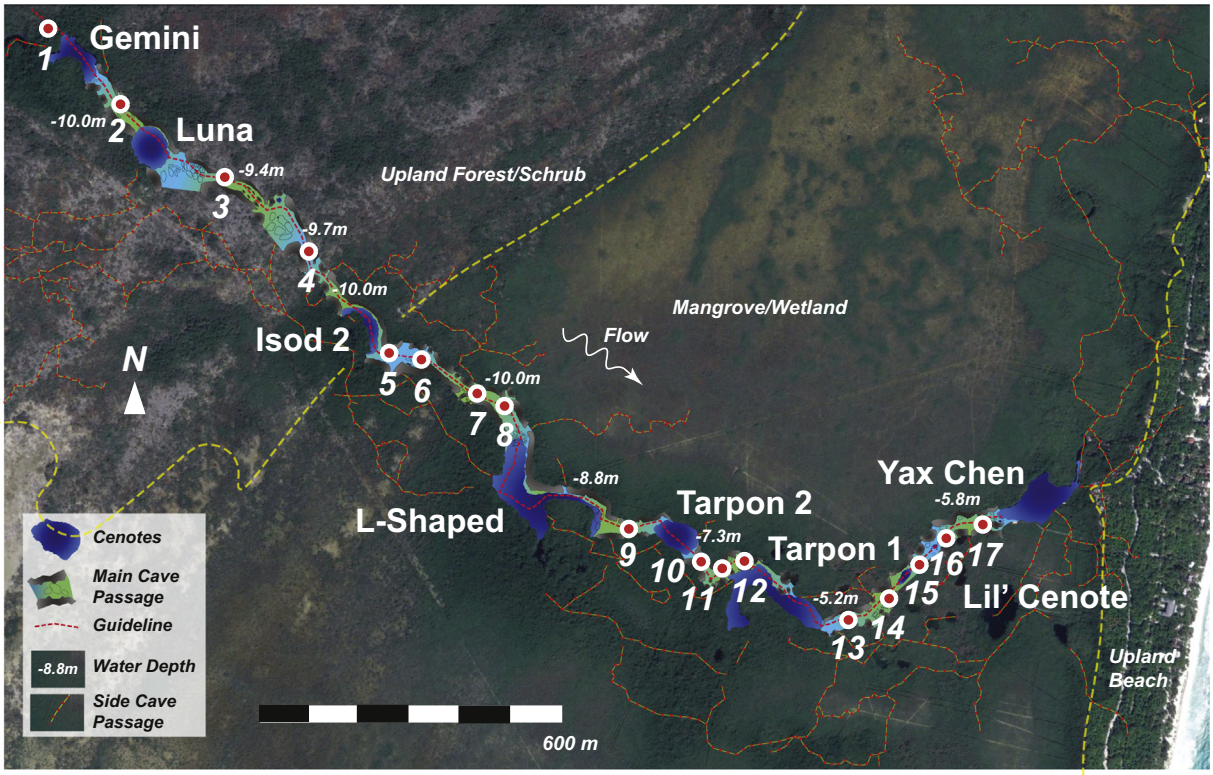

Fig. 2. Sidewall map of Yax Chen Cave System showing the cenotes and connecting cave passage with the sediment trap stations. Smaller red and yellow dashed lines represent sidewall passages which have not been mapped in detail. The mangrove/wetland transition to the upland forested/shrub terrain is also demarcated as in Fig. 1B. (For interpretation of the references to colour in this figure legend, the reader is referred to the web version of this article.)

Bel Ha cave system and elsewhere (Coutino et al., 2017; Kovacs et al., 2017; Brankovits et al., 2018; Kovacs et al., 2018). Because the Yucatan Peninsula lacks major surficial fresh water sources, the MeWM is the main source of water for the local population as well as tens of millions of vacationers who annually visit the region. The Yucatan aquifer system is one of the most extensive transboundary anchialine aquifers in the world, with 165,000 km^2 covering the Yucatan Peninsula regions of Mexico, Guatemala and Belize (Bauer-Gottwein et al., 2011). Decades of widespread tourism and coastal development have created long-term logistical concerns for wastewater and groundwater management in the highly sensitive unconfined aquifer (Molina et al., 2001; Escolero et al., 2002; Beddows, 2004; Bauer-Gottwein et al., 2011).

Because the MeWM is rain-derived, it has low salinity, dissolved solids, and ions (Beddows, 2004; Stoessell and Coke, 2006). Specific Electrical Conductivity (SEC) of the MeWM is low (< 2.5 mS/cm) and decreases moving inland from the coast (Beddows, 2004). The Total Dissolved Solid (TDS) and ion concentration is generally low as well, other than in areas where there is carbonate dissolution, marine water intrusion, or concentration due to evaporation (Smith et al., 2002; Beddows, 2004; Stoessell and Coke, 2006; Perry et al., 2009).

Groundwater flow in the Yucatan aquifer is decoupled, with the cooler MeWM (~25 °C) and warmer MaWM (~27 °C) moving in opposite directions (Beddows, 2004; Stoessell and Coke, 2006). The MeWM typically flows towards the coast at a velocity of approximately ~2.32 ± 5.21 cm/s and has been measured specifically in Ox Bel Ha at ~8–10 cm/s and increasing to 25–30 cm/s during large rainfall events (Beddows, 2004; Brankovits et al., 2018). The MaWM flows inland at a much slower rate of approximately 0.86 ± 0.52 cm/s (Beddows, 2004). There are also observations of saline intrusion inland during drought, when the regional hydraulic head is not forceful enough to create outflow from the submarine groundwater vents (Parra et al., 2016). Water table height in the Yucatan Peninsula is controlled by seasonal trends in rainfall (Marín et al., 2004; Collins et al., 2015a; Kovacs et al., 2017; Kovacs et al., 2018). Water table data recorded in the Tulum region shows broad variation in height with tidal fluctuations, dryness, and storm induced rainfall (Collins et al., 2015a; Coutino et al., 2017; Kovacs et al., 2017; Kovacs et al., 2018). Some recharge events are so large that they can periodically raise the water table on the order of meters for a number of days (Marín et al., 2004; Collins et al., 2015a; Kovacs et al., 2017; Kovacs et al., 2018). For example, the passing of Hurricane Ingrid in 2013 and Tropical Storm Hanna in 2014 resulted in variable increases in water table height (~1 m) which lasted days to weeks after the event, as excess rainwater slowly discharged at the coast (Collins et al., 2015a; Coutino et al., 2017; Kovacs et al., 2017). During rainfalls, increased flow in the MeWM causes marine water entrainment at the halocline and increases aquifer salinity as it moves towards the coast (1–2 ppt; Escolero et al., 2002; Coutino et al., 2017; Kovacs et al., 2017; Brankovits et al., 2018).

2.3. Yucatan climate

The Yucatan Peninsula has a warm, dry, evaporation dominated climate (Metcalfe et al., 2000). Seasonal variation in rainfall is prominent and is primarily controlled by the north or southward movement of the Inter Tropical Convergence Zone (ITCZ; Magaña et al., 1999). Average rainfall for the Yucatan Peninsula ranges from 550 to 1500 mm/yr, though values from 700 mm (Wilma in 2005) to over 1000 mm (Ingrid, in 2013) can be associated with the passing of large storms and hurricanes (Bauer-Gottwein et al., 2011; Farfán et al., 2014; Collins et al., 2015a; Coutino et al., 2017; Kovacs et al., 2017, 2018). There is a notable east-west rainfall gradient driven by higher rainfall along the Caribbean coast of the peninsula (> 1500 mm/y; Neuman and Rahbek, 2007). Localized storms can cause variability in the spatial patterning of rainfall, and can deliver up to 80% of annual rainfall during the summer season (González-Herrera et al., 2002). Though the Yucatan Peninsula is generally warm and dry from November to May,

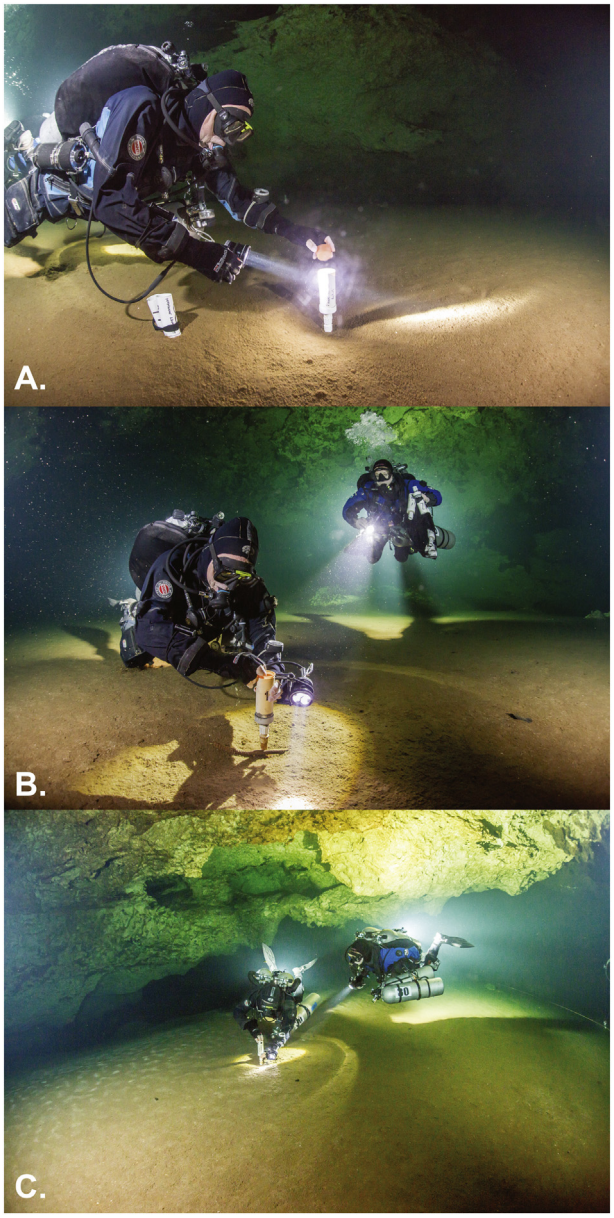

Fig. 3. Sediment trap recovery includes placing a cap on the trap prior to removal, followed by replacement of the new trap. Good buoyancy control on the part of the diver is necessary to prevent resuspension of the loose OM flocs of sediment and placement of the cap immediately upon approach prevents any percolation from entering the trap. Percolation is caused by the diver's exhalent bubbles dislodging limestone particles from the cave ceiling which fall to the cave bottom.
(Photo: Peter Gaertner.)

occasional winter storms and strong seasonal winds may occur from November to February. A "double peaked" rainy season begins in June and continues until the hurricane season occurs in September–November (Magaña et al., 1999; Boose et al., 2003; Brown et al., 2013; Farfán et al., 2014).

2.4. Yax Chen cave system

Yax Chen is a 2.7-km-long coastal subsection of the longer Ox Bel Ha cave system (270 km; Quintana Roo Speleological Survey, 2019), which is ~9 km south of Tulum. Research on this cave system was conducted by Collins et al. (2015a, 2015b), who investigated the onset of sedimentation, as well as external controls on sediment flux and composition within the cave passages (Fig. 2). The cave network trends northwest and there are 7 large cenotes (1600–9000 m^2) along the Yax Chen portion of the cave system which are surrounded by fringing and dwarf mangrove (*Rhizophora mangle, Avicennia Germians, Laguncularia racemosa*) in the downstream section and forest in the upstream reaches (Meacham, 2012; Collins et al., 2015a). The downstream vs upstream classification used for this system is based on a transition from large, mangrove-dominated cenotes in the coastal reaches, to the relatively smaller, forest dominated inland zone which occurs ~ 100 m upstream of cenote ISOD 2 (Fig. 2). The main passage of Yax Chen is generally shallow, with a depth of 10–11 m upstream of L-Shaped cenote and ~ 8 m in the downstream section. The water column within Yax Chen is stepped, with haloclines defining each water mass. Here, we define the MeWM as the upper portion (0–11 m depth) which has a salinity of ~6 ppt, and the MaWM includes an intermediate portion at ~17 ppt (11–15 m depth) and the basal marine water that intrudes from the coast (> 15 m depth ~35 ppt; Kovacs et al., 2017). Water level in the system responds to tidal fluctuations, drought periods and seasonal rainfall, including extreme events such as Hurricane Ingrid (2013), which rose the water table by ~0.75 m in Yax Chen. (Coutino et al., 2017; Kovacs et al., 2017).

The Yax Chen cave system has a substantial accumulation of organic sediment, and sedimentation within the cave is primarily controlled by productivity within adjacent cenotes and the presence/absence of mangrove (Collins et al., 2015a). The presence of large cenotes surrounded by mangrove contributes to higher bi-annual sedimentation rates in the downstream section of the cave following the rainy season (Collins et al., 2015a). Sediment flux in the upstream section of the cave (station 1 to 8) is significantly lower (0.014 mg/cm^2/day) than the downstream section (0.22 mg/cm^2/day) (Fig. 2.). Large rainfalls can induce instantaneous physicochemical changes and increase flow within the conduits, but significant impact on sedimentation is lagged by ~6–12 months (Collins et al., 2015a). However, as noted in Collins et al. (2015a), increased flow during high rainfalls does not appear to cause significant resuspension of sediment, as no obvious scour marks were observed in the sediment after the large influx of water during Hurricane Ingrid.

3. Methods

3.1. Sediment trap placement and collection

Sediment traps have been used in lakes, estuaries and oceans to determine biological and chemical fluxes in aqueous environments for over 100 years (Gardner, 1980a). The goal of most sediment trap studies is to use the bulk organic and elemental data to understand nutrient cycling and sediment composition within the water column (Gardner, 1980a; Urban et al., 2004). However, there are only a few studies where sediment traps are used to inform paleolimnological applications (Teranes and Bernasconi, 2000; Rioual et al., 2009; Collins et al., 2015a, 2015b). In 2011, fifty-one traps were placed at seventeen stations along the Yax Chen cave system to identify downstream effects of cenote size and vegetation coverage (Collins et al., 2015a). Placement was intended to document the controls of cenote size and vegetation on downstream sedimentation. The traps are constructed from PVC tubing following the design and dimensions of Gardner (1980a, 1980b). At each station, traps are placed in groups of three spanning the width of the cave and are located just above (~30 cm) the sediment-water interface (Fig. 3). See Collins et al. (2015a) for further detail on the construction, placement and collection of the sediment traps. The traps have been collected bi-annually by cave-trained SCUBA divers every May and December since May 2012. Data spanning the 2013–2017 collection period is included in this analysis.

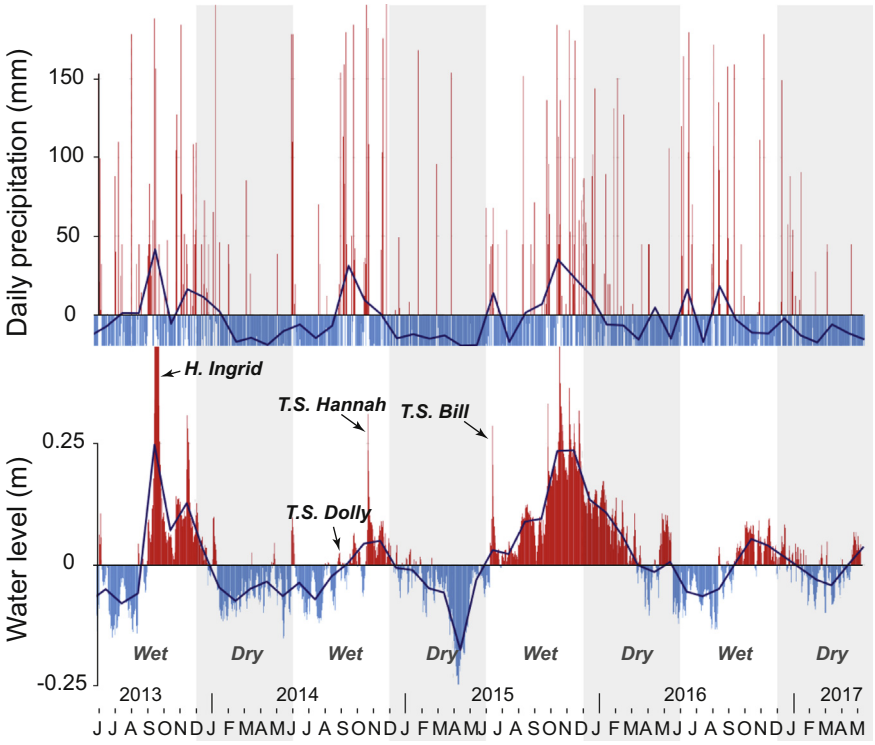

Fig. 4. Daily rainfall from the Cozumel Weather Station shown as departure from the mean over the analysis period (mm) with monthly mean (dark blue line). Below is daily water level in Yax Chen also shown as departure from mean over the analysis period (m) with the monthly mean (dark blue line). Positive and negative departure from mean water level are shown in red (positive) and blue (negative). Sediment trap collection periods and the wet/dry season are in grey shading along with notable large rainfall events (hurricanes and tropical storms). (For interpretation of the references to colour in this figure legend, the reader is referred to the web version of this article.)

3.2. Rainfall and water level data

Daily weather data (2013–2017) was collected from the Cozumel weather station as in Kovacs et al., 2017. Water level data (± 1.3 cm) was collected at 30-min intervals with a ReefNet Sensus Ultra dive logger fixed in the MeWM near station 7 and was corrected for atmospheric barometric change using a surface deployed sensor (Kovacs et al., 2017;Fig. 2). Depths (m) and rainfall (mm) are shown as departures from mean water level over the analysis period.

3.3. Sediment flux data

Bi-annual sediment flux (mg/cm^2/day) for each station was measured to document the influence of seasonal rainfall on sedimentation within Yax Chen using the methods described in Collins et al. (2015a). Sediment flux data from May 2011 to May 2014 are shown in Collins et al. (2015a), and here we include new data from June 2014 to May 2016.

3.4. μXRF core scanning

Sediment traps were recovered every six months (June–November, December–May) for 4 years (2013–2017) and the water was filtered (20 μm paper filters) to concentrate the sediment. Three sediment traps from each station were subsequently combined and homogenized through stirring as a moist paste. Samples were then loaded in a Sequential Sediment Reservoir (SSR) using a spatula, evenly compacting the sediment to ensure no void spaces were present in the ~1 cm^3 cuvette (Gregory et al., 2017). Each sequential cuvette was analyzed using the Cr heavy element (Cr-HE) X-ray source (30 Kv, 28 mA, exp. time = 15 s, step-size 1 mm) on a Cox ITRAX μXRF-CS at the McMaster University Core Scanning Facility (MUCS). Ten measurements from the central portion of each sample reservoir were averaged and the standard deviation was calculated to document variability. Data is shown as total counts over the 15 s integration time.

A subset of elements that are commonly used as weathering/lithological or biological productivity proxies were used in the PCA analysis using R's default function prcomp(). Each entry was normalized using the default scaling function and the data was subset to elements of interest (Mg, Al, Si, K, Ca, S, Ti, V, Fe, Ni, Cu, Zn, Sr) highlighted in Croudace and Rothwell (2015). Consideration of elemental abundance (i.e. high counts) relative to the variability of the measurements (standard deviation) was used to further narrow the elements of interest to Si, K, Ca, S, Fe, and Sr.

4. Results

4.1. Rainfall and groundwater level

Over the four years (June 2013 to May 2017) there were variable amounts of rainfall (Fig. 4). As described in Kovacs et al. (2017), there is a welldefined positive relationship between Cozumel rainfall and groundwater level in Yax Chen (r = 0.79, p(a) < 0.01, Fig. 9). In terms of seasonal patterning, the 2013 wet season had extensive rainfall, though it occurred late in the season (Fig. 5) and included several large events such as Hurricane Ingrid (Beven, 2014). Relatively dry conditions followed in 2014 and 2015 with a limited wet season but did have several large events (Tropical Storms Dolly and Hannah). The 2015 wet season had frequent smaller rainfalls but also several large events which peaked in October–November, and extended into 2016 (March), which is unusual compared to the other years. The 2016 wet season, like that of 2014, was short and did not have any large rainfalls (Fig. 5). As will be discussed, there is generally good correspondence between the sediment trap collection periods and the wet/dry seasons, though there are some notable deviations from this trend.

4.2. Sediment lithology

Trap samples consisted of Organic Matter (OM) rich sediment (gyttja) and were sieved at 45 μm before being examined using a dissecting binocular microscope at ~80× magnification. Components included abundant diatoms, opaline spicules and OM flocs, and to a lesser degree, particles of calcite and tan-coloured particles of limestone. In April 2019, a plankton tow (32 μm mesh) was collected from

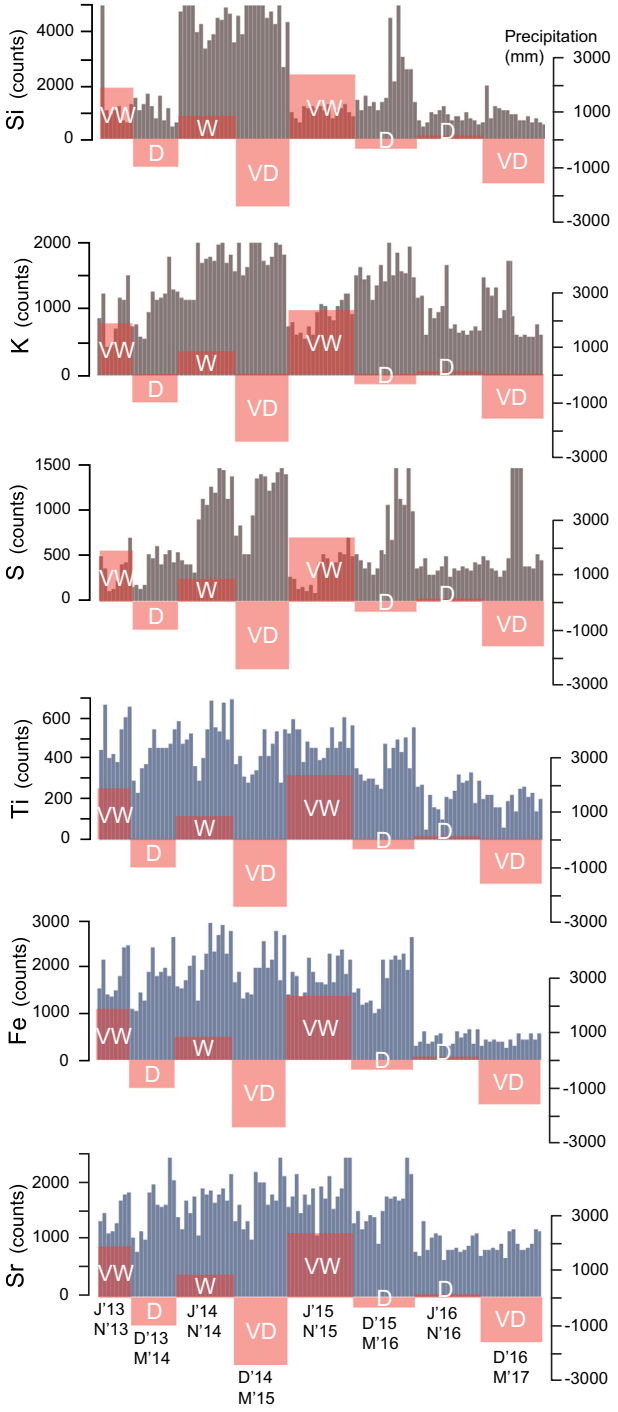

Fig. 5. Sediment trap XRF results from the eight collection periods spanning 6 months, with notation of month and year (J- June, N- November, D- December, M- May). Rainfall over the collection periods are reported in deviation from mean in mm as in Fig. 4 and relative notations indicate very wet (VW), wet (W), dry (D) and very dry (VD) seasonal periods. Biogenic influenced elements (Si, K, S - Brown; see text for discussion) as well as lithogenic elements (Ti, Fe, Sr - Blue) are shown. Station values are plotted from upstream (L) to downstream (R) for each collection period. (For interpretation of the references to colour in this figure legend, the reader is referred to the web version of this article.)

Yax Chen cenote (~3 m water depth) and was examined for its diatom content. Analysis of a wet mounted sub-sample showed an abundance of diatom frustules (50–60%) relative to other particles (undifferentiated OM). Further research will provide better estimates of

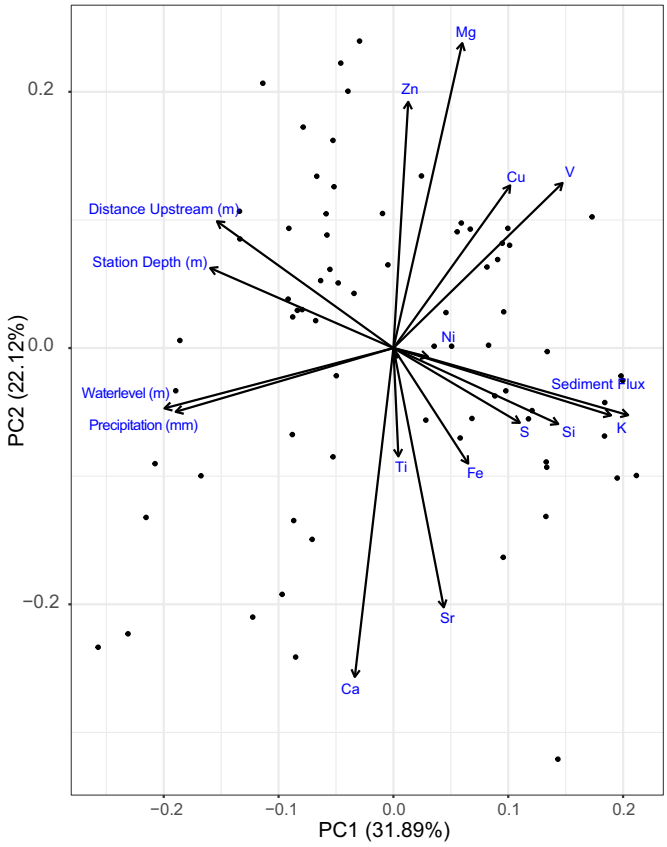

Fig. 6. Principle Components Analysis shows first two components (PC1 and 2) encompass ~54% of the data variability. Biogenic influenced elements (Si, K, S) strongly correlate with sediment flux which has an inverse relationship with station distance and depth. Lithogenic elements show intercorrelations (Ti, Fe, Sr), but do not correlate directly with water depth.

diatom content and species identification, but these preliminary results do corroborate with our high amount of Si found in the sediment trap samples. Calcareous foraminifera (*Ammonia* spp., *Elphidium*, spp.) and agglutinated taxa (testate amoebae - *Centropyxis* spp.; foraminifera - *Trochammina* spp.) were also present. Though this study did not estimate OM content (LOI), Collins et al. (2015a) found that sediment downstream from the L-Shaped Cenote had higher LOI (40–42%) than upstream (18–20%) due to the higher frequency, and surface area of the cenotes, as well as the presence of mangrove.

4.3. Element distributions

Overall, there are both temporal and spatial variations in the elemental distributions throughout the study period (Fig. 5). Elements of interest were further grouped into lithologically derived (Ti, Fe, Sr) and biologically influenced elements (K, S, Si). Although these have some overlap in terms of their origins and inputs, based on the PCA analysis and other aspects that will be discussed, these groupings of elements do seem to be largely sourced from either limestone/soil and OM or biological productivity (Fig. 6). Provenance and controls of elements will be discussed further in Section 5.1. Over the four-year study period, the biologically influenced elements tend to be highly variable and almost binary in response, with a large increase from June 2014 to May 2015, specifically in Si and S (Fig. 5). There is less variability observed in lithogenic elements, though there is a distinctive decline in the June 2016 to May 2017 collection periods ($n = 2$) following the pattern of reduced rainfall observed in Fig. 5.

The crossplots in Fig. 7 indicate that biogenic (K, S, Si) and lithogenic (Ti, Fe, Sr) elements all have strong positive relationships. K

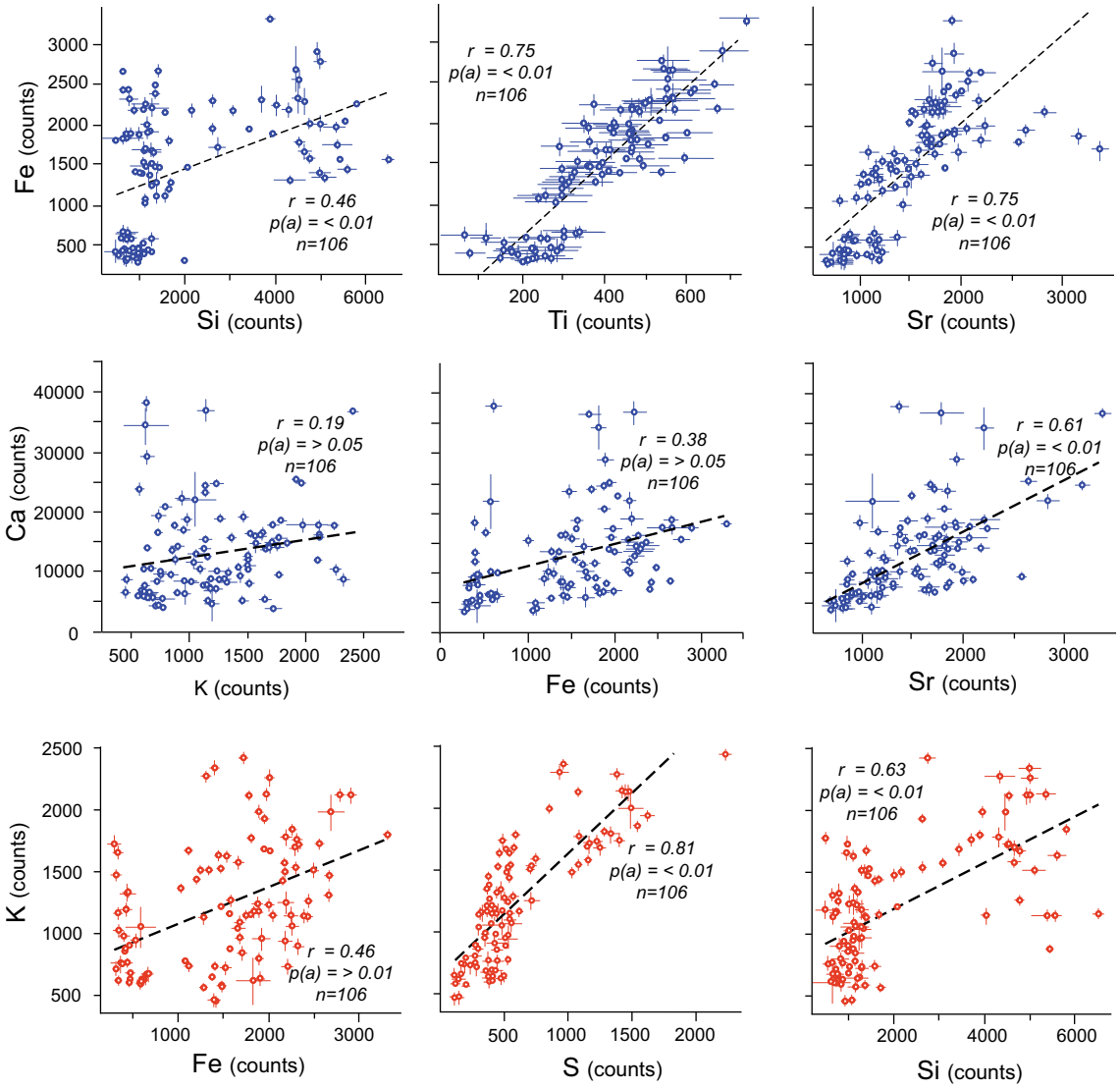

Fig. 7. Crossplots showing relationships between lithologic (blue) and biogenically influenced elements. Error bars represent standard deviations of the analysis mean for each sample cuvette. (For interpretation of the references to colour in this figure legend, the reader is referred to the web version of this article.)

correlates well with S ($r = 0.81$. p(a) < 0.01) which is a known indicator of organic matter and organic matter decay. Ca generally has poor correlations (except with Sr, $r = 0.61$, p(a) < 0.01, Fig. 7), which is likely due to both lithological and biological sources (e.g. limestone pieces, shells) within the sediment. The PCA plot (Fig. 6) shows distinct groupings in the elements of interest (Mg, Al, Si, K, Ca, S, Ti, V, Fe, Ni, Cu, Zn, Sr), with smaller groupings of lithogenic (Ti, Fe, Sr), and biogenically influenced clusters (K, S, Si, sediment flux). Distance upstream and depth of station are both orthogonal to sediment flux (Fig. 6).

Rainfall and water level in Yax Chen correspond very well to sediment flux (Kovacs et al., 2017, Collins et al., 2015a, 2015b), though comparison of elements with rainfall show variable relationships (Fig. 9). Generally, the biogenic elements are poorly correlated to rainfall, however this is likely due to time-lags associated with biological growth that complicate the temporal relationship (discussed further in Section 5.3). Overall, there is an inverse tendency towards higher element counts with lower than average rainfalls, and vice versa. This inverse relationship with rainfall is shown with sediment flux in Collins et al. (2015a), and was attributed to the lagged response of sedimentation to extreme rainfalls as a result of delayed drainage and high water tables. Individual elements show little relationship with rainfall, except for Ti ($r = 0.52$, p(a) > 0.05 overall, $r = 0.60$, p(a) > 0.05 for station 14) and S ($r = -0.62$, p(a) > 0.05). A similar trend was found in a range of Yucatan sediments by Roy et al. (2018), who suggest that elemental proxies of rainfall for the region should be ratioed with Ca rather than used individually. Upstream or downstream location and timing of rainfall relative to collection periods seem to have an impact on the overall correlation between rainfall and element counts. Local response of sediment sources and input pathways may also be affecting trends, though this is likely negligible as the study area covers a short distance (2.7 km). These factors are likely the reason for some poor correlations, as overall trends with rainfall seem predictable and individual locations seem to have slightly better relationships (e.g. Ti for station 14; Figs. 5, 9).

5. Discussion

5.1. Source and controls of weathering product and nutrients

In the Yucatan, karstification results in the accumulation of thin, patchy fine-grained soils (i.e, Leptosols, Regosols, Vertisols) that commonly contain Ca, Fe, Sr, K and Ti but also fine-grained terra rossa soils with concentrations of Al, Si and Fe oxides (Calvert and Pedersen, 2007;

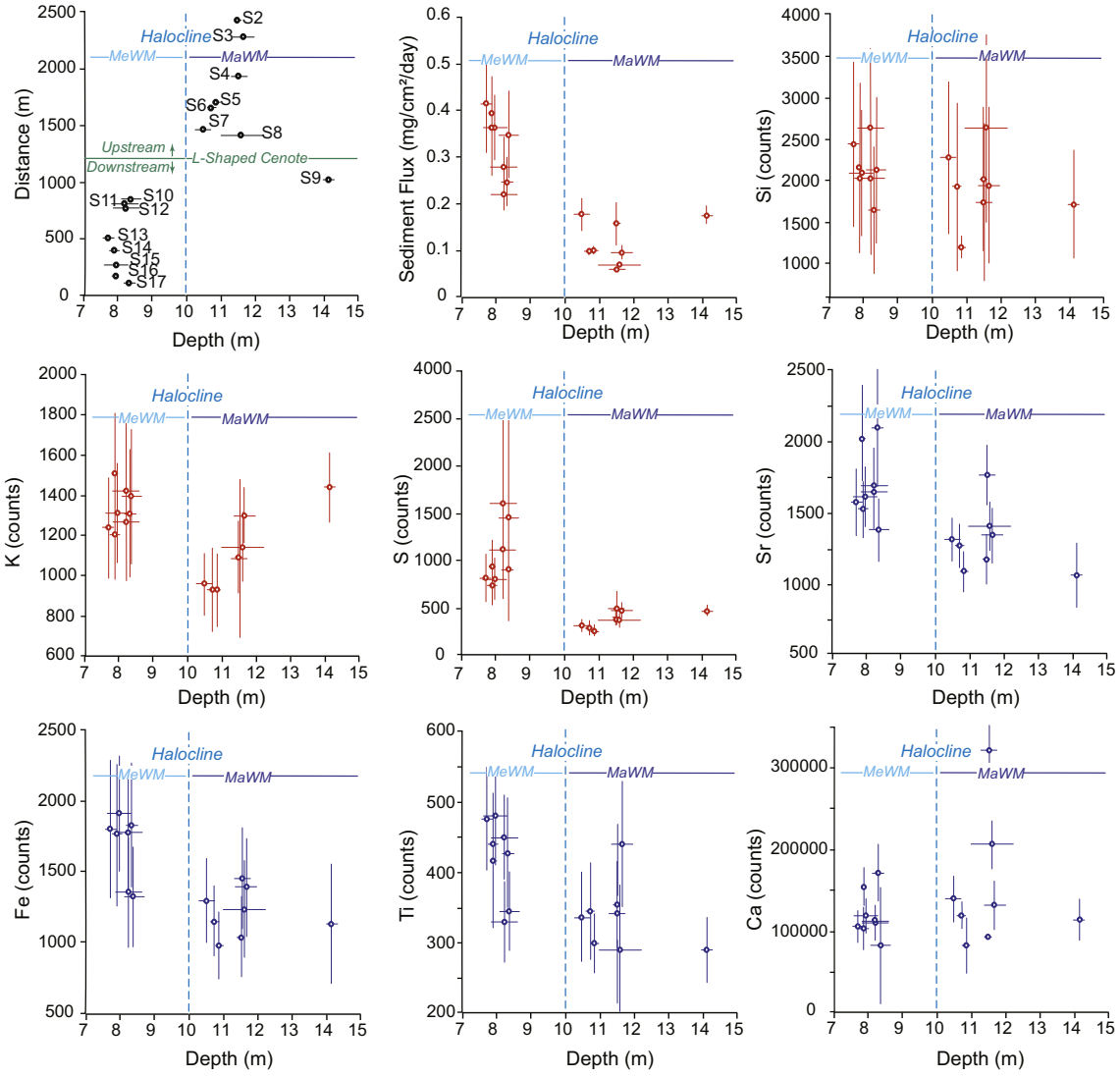

Fig. 8. Crossplots showing relationships with station depth with all parameters averaged over the study period (4 years). 1) Upstream distance along the cave passage from the Yax Chen Cenote; 2) Sediment Flux; 3–5) Biogenic influenced elements; and 6–9) Lithologic elements. Error bars represent the variation in depth for each station (n = 3 sediment traps) and the variability (standard deviation) in sediment flux and elements over the analysis period.

Cabadas et al., 2010; Bautista et al., 2011; Gaillardet et al., 2018; Roy et al., 2018). It is this process of weathering and its input via rainfall that seems to be contributing to the temporal trend in our sediment trap results. Roy et al. (2018) found that K, Ti, and Fe had only weak relationships with rainfall, but they used surface samples from lakes which were likely biased in terms of differential time averaging. Here we show that our higher temporal resolution sediment trap data that Ti/K and Si/Ti may prove to be worthwhile proxies of rainfall.

K/Ti is commonly used as a proxy for weathering rates with K as a proxy for soil weathering (clays) and Ti as a clastic sediment indicator. However, in this study, we have found the inverse relationship to be stronger, where Ti/K is strongly correlated with rainfall because there is little clay observed in the sediment and source soils are clay poor (Revel et al., 2017; Roy et al., 2018). Ti is likely derived from a limestone weathering source and present as oxyhydroxides like Fe, which are then flushed into the cenotes from flooded land areas and the mangrove with rainfall. K, which has a limestone source, but also a biologically influenced contribution from the mangrove and primary productivity in the cenotes, has a slightly time-lagged response and increases during dry periods when Ti is lower, thus emphasizing the response to rainfall and making the ratio more sensitive (Ti/K r = 0.759, p(a) > 0.05 Fig. 11). Other studies in the region have indicated that individual elements tend to be variable within sites, which can complicate the relationship with rainfall (Roy et al., 2018). For example, Roy et al. (2018) identified K/Ca as a more reliable recorder of rainfall because of the regional carbonate geology. However, due to the abundance of carbonate shell material in the cenotes and poor correspondence of Ca with other elements, this ratio was not useful in identifying trends in Yax Chen as Ca seems to be also affected by variable benthic productivity (i.e. foraminifera, gastropod shells). Relating the geochemistry of surface samples with long term spatial averages of rainfall can be useful, but does not allow for examination of the relationship with the pattern of rainfall (seasonal quantity and rates) which seems to be important as we show here (Roy et al., 2018).

Biogenic silica (SiO_2) is an indicator of diatom abundance in lacustrine sediment, and the contribution from siliciclastic sediment is often isolated effectively with Si/Ti or Si/Al (Johnson et al., 2011; Liu et al., 2013). In our data, K, S and sediment flux show similar responses to Si, indicating a shared biological influence, since the PCA and cross plots show S and Si are well correlated to K (r = 0.81, p(a) ≤ 0.01, and r = 0.63, p(a) ≤ 0.01 Figs. 6, 7). During decomposition of mangrove leaf litter, the greatest total loss is for K, with up to 95% lost within 2 weeks of inundation (Steinke et al., 1993; Kathiresan and Bingham, 2001). K and S are associated with nutrient rich particulate organic

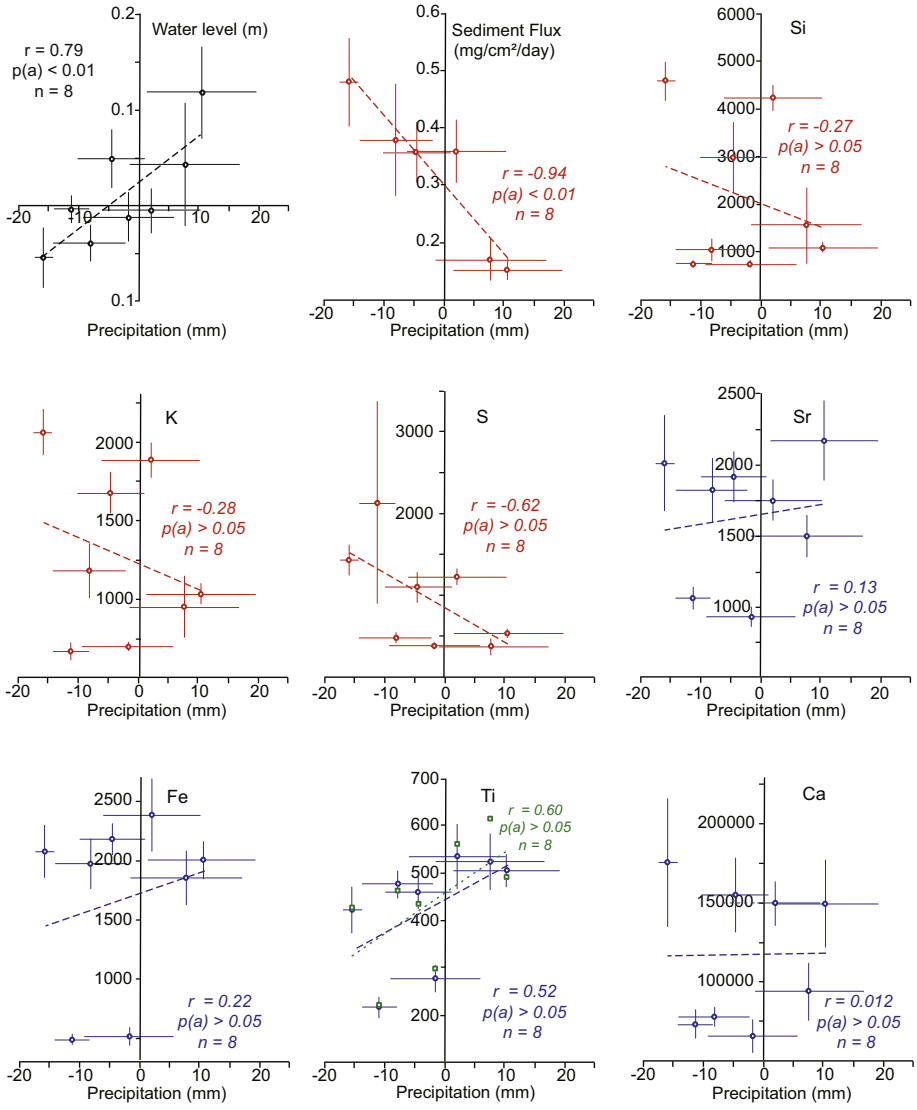

Fig. 9. Crossplots showing relationships with average precipitation (deviation from mean; mm) over the collection intervals (6 months). 1) Mean water depth (deviation from mean; m); 2) Sediment flux; 3–5) Biogenic influenced elements (red); and 6–9) Lithologic elements (blue). Error bars represent the variation in monthly precipitation over the collection periods, and the variability (standard deviation) of sediment flux and elements for all the stations (2–17) for each collection period. Green symbols and trendline (Ti) are individual values for Station 14. (For interpretation of the references to colour in this figure legend, the reader is referred to the web version of this article.)

matter (POM) derived from mangrove peat (Clark et al., 1998; Kathiresan and Bingham, 2001; Thomson et al., 2006). S is closely linked to OM and organic-rich muds, and is a product of oxidizing conditions that occur when mangrove is waterlogged (Clark et al., 1998; Croudace et al., 2006; Bayen, 2012). It is associated with the biomass of marine plants and bacterial reduction, and can be bound within organic rich muds (Ivanov, 1981; Croudace and Rothwell, 2015). Most mangrove sediment contains high levels of reduced inorganic S in the form of pyrite (FeS_2) and elemental S (Kristensen et al., 2008).

In the case of coastal Yucatan Peninsula, Si/Ti is a good candidate for estimating biogenic silica, with higher ratios indicating increased amounts of biogenic silica vs clastic or oxyhydroxide inputs (Brown, 2015). This ratio works well as a productivity proxy because siliciclastics and clays are not prevalent in the karst terrain, and the majority of Si is attributable to diatom and other phytoplankton productivity (Sánchez et al., 2002). The sediments from soils and mangroves are transported after large rainfalls when groundwater level drops causing overland flow into adjacent cenotes, and through cracks and fissures. This flow introduces a significant load of nutrients into the sunlit cenotes, where primary productivity occurs in the drier months after the events which is then transported downstream into the cave conduits. This is discussed further in Section 5.3.

5.2. Spatial and temporal variation in element trends

There are site-specific variations in elemental trends based on cenote characteristics such as vegetation coverage (mangrove vs. forest), position upstream or downstream of L-Shaped Cenote, and cenote surface area. As described in Collins et al. (2015a), there is a relationship with higher sediment flux in downstream locations (station 5 to 17) vs upstream, which is likely due to mangrove coverage and the predominance of large surface area cenotes in the downstream reaches of the cave. However, there is also a notable change in cave bottom depth between the upstream and downstream sections, resulting in the halocline being closer (or below) the cave bottom in the upstream areas. Phytoplankton and OM particulates/flocs may be preferentially deposited on the cave bottom in the downstream areas because the cave bottom is within the less dense MeWM versus the upstream areas which are at, or below the halocline. Because of the large water density change, fine OM flocs may not readily settle through the MaWM. The average elemental values (K, S, Sr, Fe, Ti) for each station and their standard deviations over the analysis period (4 yrs) show a tendency towards lower values upstream of the L-Shaped cenote which is reinforced with the PCA suggesting that distance and depth are both influencing distribution of these elements (Fig. 8). The station averages for Si over the analysis period however, showed no trend upstream, but PCA on station data (6 months collection period) was found to be

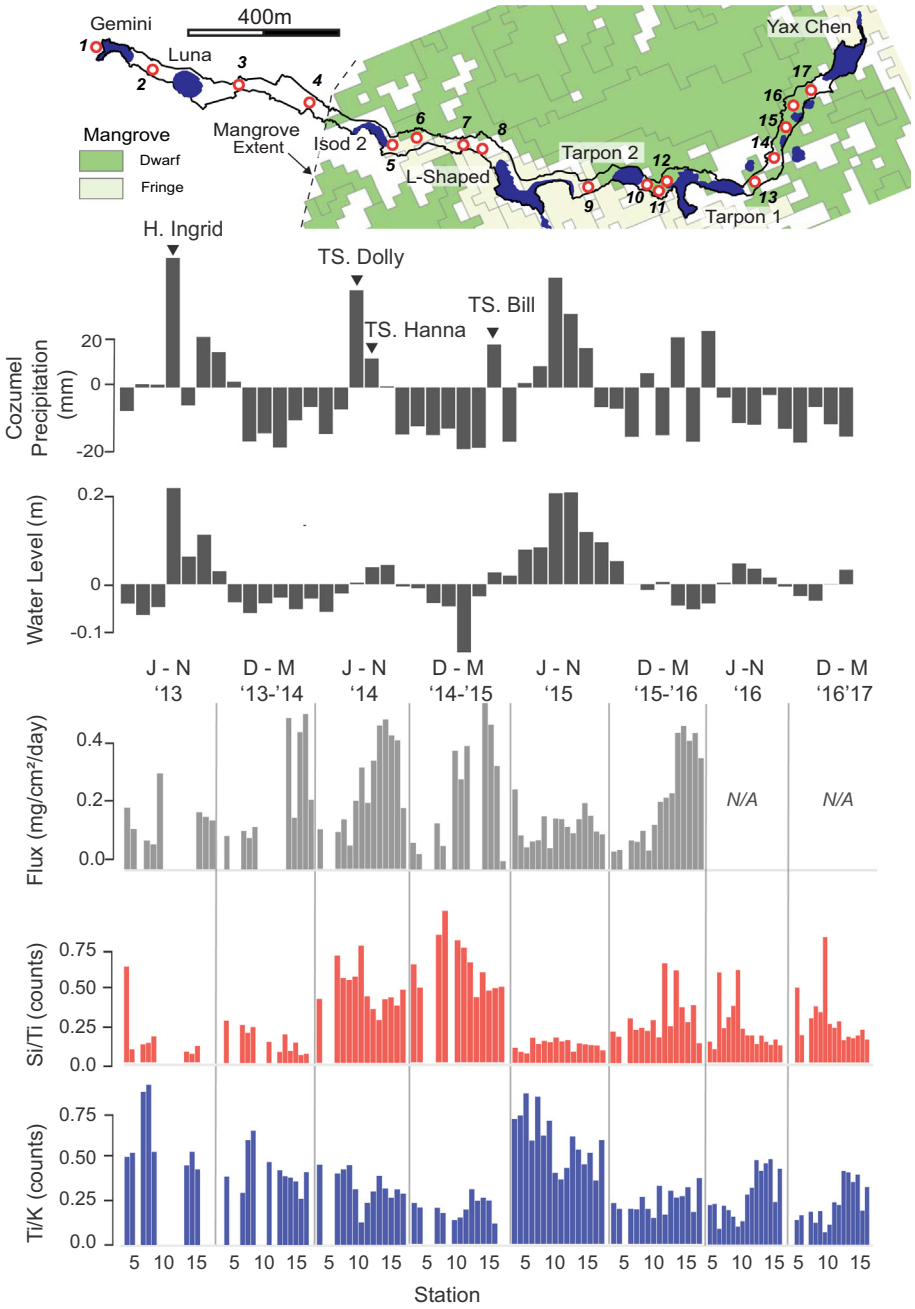

Fig. 10. Map of Yax Chen cave system with locations of sediment collection sites and mangrove coverage (top). Cozumel precipitation (in mm) and water level in Yax Chen (in m) are indicated with dark grey bars representing monthly collection. Sediment flux (light grey- sediment amount in g/cm^2), Si/Ti (red - biogenic proxy), and Ti/K (blue - lithogenic proxy) are arranged by collection period and station location as in Fig. 5. (For interpretation of the references to colour in this figure legend, the reader is referred to the web version of this article.)

inversely related to distance and water depth. Some of the discrepancy may be related to slight matrix effects in the uXRF data as the upstream vs downstream areas have slightly lower LOI values (~10–20%) as shown in Collins et al. (2015a, 2015b), but could also be due to settling rate with the diatoms preferentially settling through the halocline vs the lighter flocs of OM. Elemental ratios reduce some of these matrix effects, but also site-specific changes in elemental inputs maybe playing a role (e.g. Gregory et al., 2019).

Increases in the lithogenic proxy Ti/K are observed from the June–November 2013 and June–November 2015 collection periods associated with the passing of Hurricane Ingrid in September 2013, and a prolonged 2015 wet season (Fig. 10). Though there is no increase in the biogenic proxy Si/Ti from the 2013 hurricane period (June–November 2013), there is a large increase during June–November and December–May 2014–15, which were relatively dry periods, but also included several tropical storms (Dolly, Hanna, Bill). Likewise, Si/Ti values tend to be higher after the June–November 2015 wet season. This apparent lag in primary productivity (sediment flux and LOI) after large rainfalls or wet periods was noted in Collins et al. (2015a) as a response to nutrient input and productivity in the sunlit cenotes. In this study, we find a similar response with the biological proxies Si, K and S showing a lagged response to both high and low rainfalls (Fig. 5). During high rainfalls there is increased nutrient input, but high MeWM flow limits their residence time in the sunlit cenotes, while during subsequent dry periods flow is correspondingly lower, thus allowing phytoplankton blooms (Brankovits et al., 2018). Our time

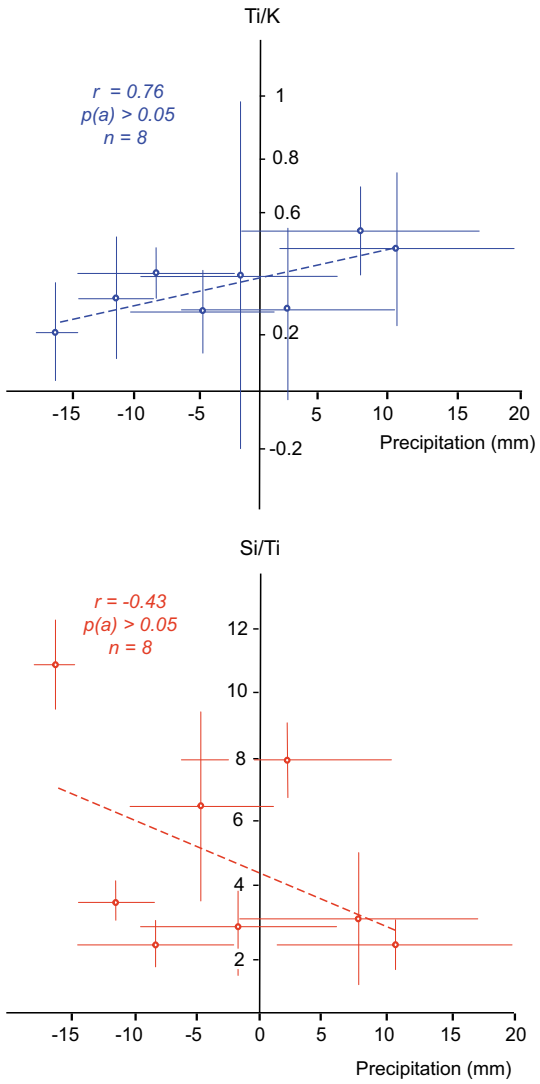

Fig. 11. Plots showing relationships between precipitation (deviation from mean; mm, m), Si/Ti which may be a useful hurricane/tropical storm indicator and Ti/K as a paleorainfall proxy.

lag in primary productivity is somewhat obscured by our 6-month collection period, but Schmitter-Soto et al., 2002 found the highest number of phytoplankton and chlorophyceans in Yucatan cenotes during the dry winter season, and time lags in biological productivity have been observed in other coastal oligotrophic lakes in Florida after hurricanes (James et al., 2008; Beaver et al., 2013). In the months after Hurricanes Frances and Jean (September 2004), percent biovolume of diatoms in Lake Okeechobee, Florida increased to over 60% in the nearshore region and over 80% in the offshore region (James et al., 2008; Beaver et al., 2013).

The large amount of rainfall during the 2015 summer wet season is not associated with a known hurricane or tropical storm but was due to frequent smaller events which caused protracted high groundwater levels. The lithogenic proxy Ti/K increases during this period like that during Hurricane Ingrid (June–November 2013), and there is a smaller, but time lagged response in sediment flux and Si/Ti in subsequent collection periods (Fig. 10). Over the four years of this study, Ti/K appears to be more sensitive to overall rainfall amounts while Si/Ti is more 'binary' in response to singular large rainfall events like Hurricane Ingrid.

5.3. 5.3 Effect of mangrove coverage on cave sedimentation

Based on the sediment trap results for the past 4 years it appears that mangrove coverage (in contrast to upland forested terrain) affects the amount and composition of sediment accumulating in downstream cave conduits, but sedimentation in the whole cave system is responding to changes in rainfall. Mangrove peat coverage adjacent to cenotes acts as an aquitard which reduces permeability and percolation of rainwater to the subsurface that is otherwise rapid in upland forest terrain because of the thin soil coverage and exposed karst (Fig. 12). The reduction in permeability due to peat occlusion of the upper karst causes ponding of water in the mangrove area which warms and leach nutrients (such as K, N, P) from the surrounding leaf litter and OM debris (Steinke et al., 1993; Li and Ye, 2014). When large rainfalls occur, or frequent smaller events, groundwater level rises and floods the surrounding terrain, which then flushes into the cenotes as water level drops after large rainfalls and into the dry season. When a large amount of rainwater enters the system (Fig. 12), high flow within the MeWM results in little to no residence time of that water in the sunlit cenotes, limiting phytoplankton productivity. In the subsequent dry period, as water level drops and MeWM flow wanes, nutrients from the mangrove water then cause increased primary productivity in the cenotes. It appears that large rainfalls with high groundwater levels are 'flushing' more nutrients into the cenotes, and smaller, but more frequent rainfalls are only causing a partial 'flushing' of mangrove water (Fig. 12).

5.4. Considerations for core locations

This study demonstrates that cave sediment geochemistry from Yax Chen reflects hydrological conditions associated with intense rainfall events and wet and dry seasons. More importantly, it highlights the spatial variability of the cave system as a sensitive recorder of paleoclimate, and provides guiding information for future coring locations and for understanding paleohydrology. Locations downstream of large cenotes and mangrove areas along with areas within the MeWM will provide the highest resolution record and will be the most sensitive in terms of recording environmental change. However, as we have demonstrated in Yax Chen, all areas (forested terrain as well as mangrove) are recording changes in rainfall, but the differences between areas in terms of sediment rate and geochemistry will be useful for understanding the effects of sea-level change (Collins et al., 2015b).

Good potential proxies include Ti/K, which is sensitive to total rainfall, and Si/Ti which is indicative of extreme rainfalls. Site specific variations may play a role in elemental response, but the pattern of change should be reproducible. Though the correlation between Si/Ti and rainfall is not as robust as Ti/K, this is likely influenced by a variable lag in response that has to do with other controls of primary productivity (such as rainfall/drought timing, heliometric heating, cenote size, etc.; Figs. 10, 11). Nonetheless, the data shows clear impacts of large rainfall events (e.g., Hurricane Ingrid, 2015 wet season; Fig. 10).

5.5. Implications for future mangrove-cenote interactions

This study has provided information on how the geochemistry of the cenote-cave environments in the Yax Chen system respond to intense wet and dry events, and how this can be identified in the paleo-record. Changing climate and warming ocean temperatures are expected to exacerbate hurricane intensity and frequency, leading to more climate uncertainty including more frequent and powerful storms and droughts that will increase the vulnerability of the aquifer to both natural and anthropogenic perturbations (Boose et al., 2003; Bauer-Gottwein et al., 2011; Farfán et al., 2014; Sobel et al., 2016). This is becoming an evermore pressing issue as mangrove forests are becoming globally one of the most threatened tropical ecosystems (Bayen, 2012; Torrescano-Valle and Islebe, 2012). Redox potential of the mangrove sediment is

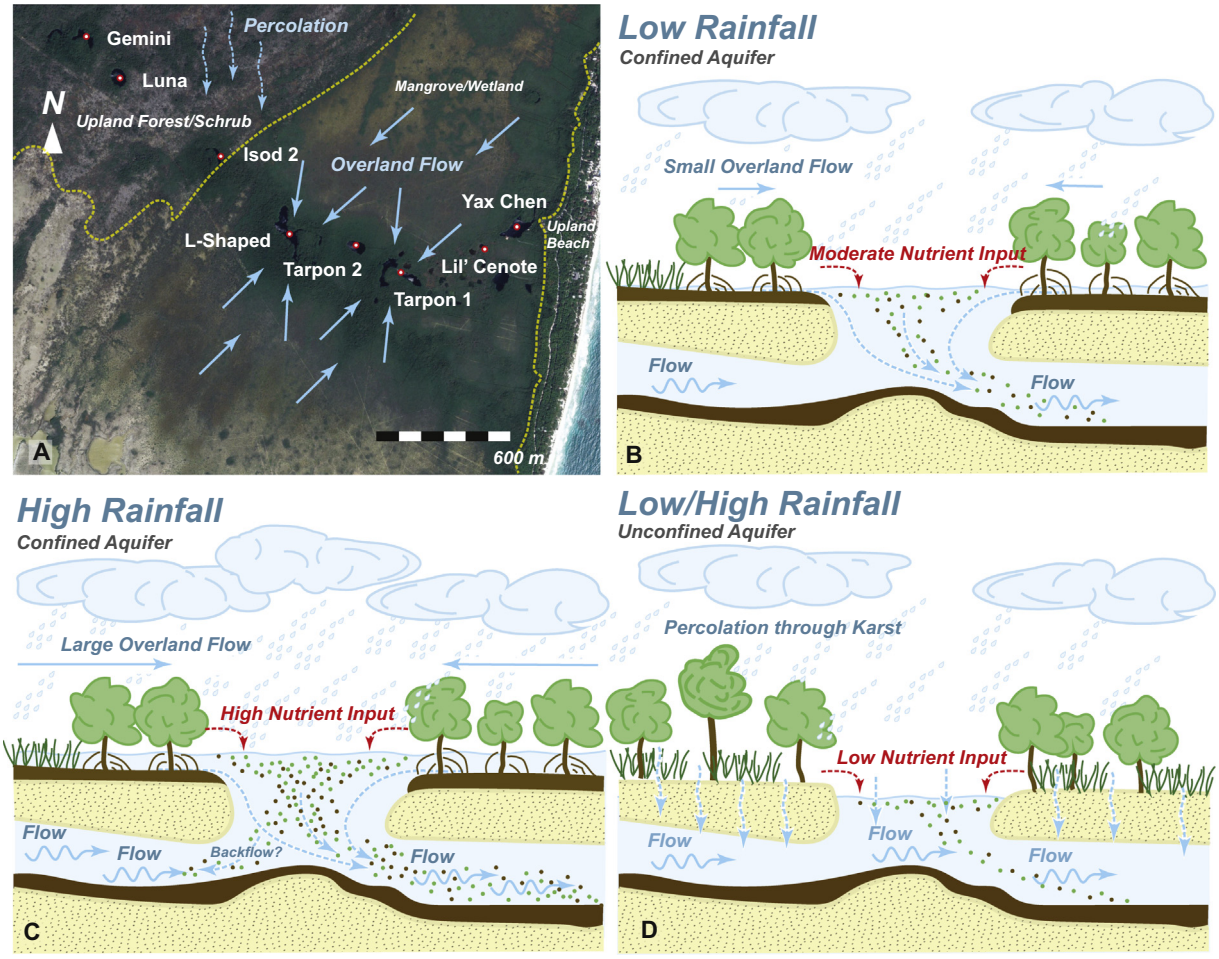

Fig. 12. Conceptual diagram showing the relationship between groundwater and rainfalls (low and high) along with differences between mangrove and upland forest/shrub terrains and their impact on cave sedimentation.

controlled by seasonal waterlogging (Marchand et al., 2011; Bayen, 2012), and provides an important control on the accumulation of many trace metals (Clark et al., 1998). Mangrove peat is naturally a heavy metal sink because mangrove roots baffle sediment and accumulate fine-grained sulphidic organic matter and heavy metals under anoxic conditions, however when heavily disturbed they become more oxic during flushing events, and thus as we show here, the peat could become a source of metals release to the aquifer and shallow coastal ocean and reef systems (Clark et al., 1998; Defew et al., 2005; Marchand et al., 2011). There are also substantial amounts of P in mangrove environments which has the potential to be mobilized into oligotrophic environments during large storms and cause harmful algal blooms (Hernández-Terrones et al., 2011). It is likely that when large storms flood and waterlog the mangrove, leaching from decomposition is enhanced, which introduces more nutrients and heavy metals into the water, which is then drained into the open water during the drier season. Human activity is quickly developing in areas adjacent to mangrove covered cenotes, which may increase the concentration of nitrates, sulphates, sulphide-bound metals and hydrocarbons in mangrove peat (Harbison, 1986; Ellison and Farnsworth, 1996; Defew et al., 2005; Kalnejais et al., 2010; Bayen, 2012). This is important to note going forward because modern groundwater management problems in many of these regions are related to long term quality and balancing impacts from development (Molina et al., 2001; Escolero et al., 2002; Hausman, 2009). Increases in coastal development, coupled with the potential for higher magnitude and frequency of hurricanes may result in a detrimental impact to the local coastal ecosystems in the future (Torrescano-Valle and Islebe, 2012). This has already been observed in the coastal region of the northern Yucatan Peninsula (Escolero et al., 2002; Hernández-Terrones et al., 2011), and in some pockets of the Mayan Riviera (Baker et al., 2010).

6. Conclusions

Broad seasonal trends (wet/dry) and large magnitude events can be defined in the sediment geochemistry of Yax Chen. Though individual elements averaged throughout the cave system did not show strong correlations (except for Ti which showed moderate relationships), in general, lithologically derived elements (Ti, Fe, Sr) fit the broad patterning of rainfall. Biologically influenced elements (K, S, Si) also showed a rainfall response representing primary productivity and mangrove derived sediment but further exhibited a lagged response to hurricanes and tropical storms. The ratio Ti/K is the most robust proxy for rainfall and shows a strong trend, while Si/Ti has a lagged response but is a good detector of large rainfall events (i.e, hurricanes and tropical storms).

This study shows how sediment geochemistry and uXRF core scanning can provide paleoclimatic records of rainfall in cave sediments but also has potential applications for lake sediments as it shows overall elemental response to rainfall. Previous research did not show a strong relationship between rainfall and lake surface sample geochemistry, but our high temporal resolution study has shown the rate and duration of rainfalls is a factor and there is variable response amongst elements with lags in timing.

Acknowledgements

The authors gratefully acknowledge the support of The Mexican Cave Exploration Project (MCEP), CINDAQ, and the staff at Zero Gravity for dive support and logistics. This research was possible through the MCEP Science Week volunteers from around the world. Special thanks go to Jan Duikt, Peter Gaertner and Manuela Schoch for repeated support each year and photography. Graham Mushet and Cecilia Barouillet from Paleoecological Environmental Assessment and Research Laboratory (PEARL) at Queen's University provided diatom analysis of the plankton tow from Yax Chen. Natural Sciences and Engineering Research Council (NSERC) Discovery Grants (EGR - 2015-057250) and the Canada Foundation for Innovation John R. Evans Leaders Fund (CFI-JELF grant 105-04523). We would also like to thank the reviewers for their helpful comments.

Appendix A. Supplementary data

Supplementary data to this article can be found online at https://doi.org/10.1016/j.palaeo.2019.109289.

References

Back, W., Hanshaw, B.B., 1970. Comparison of chemical hydrogeology of the carbonate peninsulas of Florida and Yucatan. J. Hydrol. 10 (4), 330–368.
Baker, D.M., Jordán-Dahlgren, E., Maldonado, M.A., Harvell, C.D., 2010. Sea fan corals provide a stable isotope baseline for assessing sewage pollution in the Mexican Caribbean. Limnol. Oceanogr. 55 (5), 2139–2149.
Bauer-Gottwein, P., Gondwe, B.R., Charvet, G., Marín, L.E., Rebolledo-Vieyra, M., Merediz-Alonso, G., 2011. Review: the Yucatán Peninsula karst aquifer, Mexico. Hydrogeol. J. 19 (3), 507–524.
Bautista, F., Palacio-Aponte, G., Quintana, P., Zinck, J.A., 2011. Spatial distribution and development of soils in tropical karst areas from the Peninsula of Yucatan, Mexico. Geomorphology 135 (3–4), 308–321.
Bayen, S., 2012. Occurrence, bioavailability and toxic effects of trace metals and organic contaminants in mangrove ecosystems: a review. Environ. Int. 48, 84–101.
Beaver, J.R., Casamatta, D.A., East, T.L., Havens, K.E., Rodusky, A.J., James, R.T., ... Buccier, K.M., 2013. Extreme weather events influence the phytoplankton community structure in a large lowland subtropical lake (Lake Okeechobee, Florida, USA). Hydrobiologia 709 (1), 213–226.
Beddows, P.A., 2004. Groundwater Hydrology of a Coastal Conduit Carbonate Aquifer: Caribbean Coast of the Yucatán Peninsula, México. PhD Thesis. University of Bristol, UK.
Beddows, P.A., Smart, P.L., Whitaker, F.F., Smith, S.L., 2007. Decoupled fresh saline groundwater circulation of a coastal carbonate aquifer: spatial patterns of temperature and specific electrical conductivity. Journal of Hydrology 346, 18–32.
Beven, J.L.I., 2014. Hurricane Ingrid, National Hurricane Centre Tropical Cyclone Report, Volume 2014. National Weather Service.
Bischoff, J.L., Cummins, K., Shamp, D.D., 2005. Geochemistry of sediments in cores and sediment traps from Bear Lake, Utah and Idaho (No. 2005–1215).
Boose, E.R., Foster, D.R., Barker Plotkin, A., Hall, B., 2003. Geographical and historical variation in hurricanes across the Yucatan Peninsula. In: Gomez-Pompa, A., Allen, M.F., S. F, Jimenez-Osornio, J.J. (Eds.), Lowland Maya Area:Three Millennia at the Human-Wildland Interface. Haworth Press, New York, pp. 495–516.
Brankovits, D., Pohlman, J.W., Ganju, N.K., Iliffe, T.M., Lowell, N., Roth, E., Sylva, Emmert, Lapham, 2018. Hydrologic Controls of Methane Dynamics in Karst Subterranean Estuaries.
Brown, Erik, 2015. Estimation of Biogenic Silica Concentrations Using Scanning XRF: Insights from Studies of Lake Malawi Sediments. https://doi.org/10.1007/978-94-017-9849-5_9.
Brown, A.L., Reinhardt, E.G., van Hengstum, P.J., Pilarczyk, J.E., 2013. A coastal Yucatan sinkhole records intense hurricane events. J. Coast. Res. 30 (2), 418–428.
Cabadas, H.V., Solleiro, E., Sedov, S., Pi, T., Alcalá, J.R., 2010. The complex genesis of red soils in Peninsula de Yucatan, Mexico: mineralogical, micromorphological and geochemical proxies. Eurasian soil science 43 (13), 1439–1457.
Calvert, S.E., Pedersen, T.F., 2007. Elemental proxies for palaeoclimatic and palaeoceanographic variability in marine sediments: interpretation and application. In: Hillaire-Marcel, C., De Vernal, A. (Eds.), Proxies in Late Cenozoic Paleoceanography. Elsevier, Dev Mar Geol, pp. 567–644.
Carrillo-Bastos, A., Islebe, G.A., Torrescano-Valle, N., González, N.E., 2010. Holocene vegetation and climate history of central Quintana Roo, Yucatán Península, Mexico. Rev. Palaeobot. Palynol. 160 (3-4), 189–196.
Clark, M.W., McConchie, D., Lewis, D.W., Saenger, P., 1998. Redox stratification and heavy metal partitioning in Avicennia-dominated mangrove sediments: a geochemical model. Chem. Geol. 149 (3–4), 147–171.
Collins, S.V., Reinhardt, E.G., Werner, C.L., Le Maillot, C., Devos, F., Meacham, S.S., 2015a. Regional response of the coastal aquifer to Hurricane Ingrid and sedimentation flux in the Yax Chen cave system (Ox Bel Ha) Yucatan, Mexico. Palaeogeograp. Palaeoclimatol. Palaeoecol. 438, 226–238.
Collins, S.V., Reinhardt, E.G., Werner, C.L., Le Maillot, C., Devos, F., Rissolo, D., 2015b. Late Holocene mangrove development and onset of sedimentation in the Yax Chen cave system (Ox Bel Ha) Yucatan, Mexico: Implications for using cave sediments as a sea-level indicator. Palaeogeogr. Palaeoclimatol. Palaeoecol. 438, 124–134.
Coutino, A., Stastna, M., Kovacs, S., Reinhardt, E., 2017. Hurricanes Ingrid and Manuel (2013) and their impact on the salinity of the Meteoric Water Mass, Quintana Roo, Mexico. Journal of Hydrology. 551, 715–729.
Croudace, I.W., Rothwell, R.G. (Eds.), 2015. Micro-XRF Studies of Sediment Cores: Applications of a non-destructive tool for the environmental sciences. Vol. 17 Springer.
Croudace, I.W., Rindby, A., Rothwell, R.G., 2006. ITRAX: description and evaluation of a new multi-function X-ray core scanner. Geol. Soc. Lond., Spec. Publ. 267 (1), 51–63.
Curtis, J.H., Hodell, D.A., Brenner, M., 1996. Climate variability on the Yucatan Peninsula (Mexico) during the past 3500 years, and implications for Maya cultural evolution. Quat. Res. 46 (1), 37–47.
Dauvalter, V., Rognerud, S., 2001. Heavy metal pollution in sediments of the Pasvik River drainage. Chemosphere 42 (1), 9–18.
Defew, L.H., Mair, J.M., Guzman, H.M., 2005. An assessment of metal contamination in mangrove sediments and leaves from Punta Mala Bay, Pacific Panama. Mar. Pollut. Bull. 50 (5), 547–552.
Ellison, A.M., Farnsworth, E.J., 1996. Anthropogenic disturbance of Caribbean mangrove ecosystems: past impacts, present trends, and future predictions. Biotropica 549–565.
Escolero, O.A., Marin, L.E., Steinich, B., Pacheco, A.J., Cabrera, S.A., Alcocer, J., 2002. Development of a protection strategy of karst limestone aquifers: the Merida Yucatan, Mexico case study. Water Resour. Manag. 16 (5), 351–367.
Farfán, L.M., D'Sa, E.J., Liu, K.B., Rivera-Monroy, V.H., 2014. Tropical cyclone impacts on coastal regions: the case of the Yucatán and the Baja California Peninsulas, Mexico. Estuar. Coasts 37 (6), 1388–1402.
Froger, C., Ayrault, S., Evrard, O., Monvoisin, G., Bordier, L., Lefèvre, I., Quantin, C., 2018. Tracing the sources of suspended sediment and particle-bound trace metal elements in an urban catchment coupling elemental and isotopic geochemistry, and fallout radionuclides. Environ. Sci. Pollut. Res. 25 (28), 28667–28681.
Gaillardet, J., Calmels, D., Romero-Mujalli, G., Zakharova, E., Hartmann, J., 2018. Global climate control on carbonate weathering intensity. Chem. Geol.
Gardner, W.D., 1980a. Field assessment of sediment traps. Journal of Marine Research 38 (1), 41–52.
Gardner, W.D., 1980b. Sediment trap dynamics and calibration: a laboratory evaluation. Journal of Marine Research 38 (1), 17–39.
González-Herrera, R., Sánchez-y-Pinto, I., Gamboa-Vargas, J., 2002. Groundwater-flow modeling in the Yucatan karstic aquifer, Mexico. Hydrogeol. J. 10 (5), 539–552.
Gregory, B.R., Reinhardt, E.G., Macumber, A.L., Nasser, N.A., Patterson, R.T., Kovacs, S.E., Galloway, J.M., 2017. Sequential sample reservoirs for Itrax-XRF analysis of discrete samples. J. Paleolimnol. 57 (3), 287–293.
Gregory, B.R., Patterson, R.T., Reinhardt, E.G., Galloway, J.M., Roe, H.M., 2019. An evaluation of methodologies for calibrating Itrax X-ray fluorescence counts with ICP-MS concentration data for discrete sediment samples. Chem. Geol. 521, 12–27.
Harbison, P.A.T., 1986. Mangrove muds—a sink and a source for trace metals. Mar. Pollut. Bull. 17 (6), 246–250.
Haug, G.H., Hughen, K.A., Sigman, D.M., Peterson, L.C., Röhl, U., 2001. Southward migration of the intertropical convergence zone through the Holocene. Science 293 (5533), 1304–1308.
Hausman, H., 2009. Responsible Development in Tulum, Mexico: Considering Water Quality and Subaqueous Cave Locations. Master of Environmental Management Thesis. Duke University.
Hernández-Terrones, L., Rebolledo-Vieyra, M., Merino-Ibarra, M., Soto, M., Le-Cossec, A., Monroy-Ríos, E., 2011. Groundwater pollution in a karstic region (NE Yucatan): baseline nutrient content and flux to coastal ecosystems. Water Air Soil Pollut. 218 (1-4), 517–528.
Hodell, D.A., Brenner, M., Curtis, J.H., Medina-Gonzalez, R., Can, E.I.C., Albornaz-Pat, A., Guilderson, T.P., 2005. Climate change on the Yucatan Peninsula during the little ice age. Quat. Res. 63 (2), 109–121.
Ivanov, M.V., 1981. The global biogeochemical sulphur cycle. In: Likens, G.E. (Ed.), Some Perspectives of the Major Biogeochemical Cycles SCOPE, pp. 61–78.
James, T.R., Chimney, M.J., Sharfstein, B., Engstrom, D.R., Schottler, S.P., East, T., Jin, K.R., 2008. Hurricane effects on a shallow lake ecosystem, Lake Okeechobee, Florida (USA). Fundamental and Applied Limnology/Archiv für Hydrobiologie 172 (4), 273–287.
Johnson, T.C., Brown, E.T., Shi, J., 2011. Biogenic silica deposition in Lake Malawi, East Africa over the past 150,000 years. Palaeogeogr. Palaeoclimatol. Palaeoecol. 303 (1), 103–109.
Kalnejais, L.H., Martin, W.R., Bothner, M.H., 2010. The release of dissolved nutrients and metals from coastal sediments due to resuspension. Mar. Chem. 121 (1–4), 224–235.
Kathiresan, K., Bingham, B.L., 2001. Biology of Mangroves and Mangrove Ecosystems.
Kovacs, S.E., Reinhardt, E.G., Stastna, M., Coutino, A., Werner, C., Collins, S.V., Le Maillot, C., 2017. Hurricane Ingrid and tropical storm Hanna's effects on the salinity of the coastal aquifer, Quintana Roo, Mexico. Journal of Hydrology. 551, 703–714.
Kovacs, S.E., Reinhardt, E.G., Chatters, J.C., Rissolo, D., Schwarcz, H.P., Collins, S.V., Erreguerena, P.L., 2018. Calcite raft geochemistry as a hydrological proxy for Holocene aquifer conditions in Hoyo Negro and Ich Balam (Sac Actun Cave System), Quintana Roo, Mexico. Quat. Sci. Rev. 175, 97–111.
Kristensen, E., Bouillon, S., Dittmar, T., Marchand, C., 2008. Organic carbon dynamics in mangrove ecosystems: a review. Aquat. Bot. 89 (2), 201–219.
Kylander, M.E., Ampel, L., Wohlfarth, B., Veres, D., 2011. High-resolution X-ray fluorescence core scanning analysis of Les Echets (France) sedimentary sequence: new insights from chemical proxies. J. Quat. Sci. 26 (1), 109–117.
Li, T., Ye, Y., 2014. Dynamics of decomposition and nutrient release of leaf litter in

Kandelia obovata mangrove forests with different ages in Jiulongjiang Estuary, China. Ecol. Eng. 73, 454–460.
Liu, X., Colman, S.M., Brown, E.T., Minor, E.C., Li, H., 2013. Estimation of carbonate, total organic carbon, and biogenic silica content by FTIR and XRF techniques in lacustrine sediments. J. Paleolimnol. 50 (3), 387–398.
Lo, F.L., Chen, H.F., Fang, J.N., 2017. Discussion of suitable chemical weathering proxies in sediments by comparing the dissolution rates of minerals in different rocks. The Journal of Geology 125 (1), 83–99.
Magaña, V., Amador, J.A., Medina, S., 1999. The midsummer drought over Mexico and Central America. J. Clim. 12 (6), 1577–1588.
Marchand, C., Allenbach, M., Lallier-Vergès, E., 2011. Relationships between heavy metals distribution and organic matter cycling in mangrove sediments (Conception Bay, New Caledonia). Geoderma 160 (3–4), 444–456.
Marín, L.E., Perry, E.C., Essaid, H., Steinich, B., 2004. Hydrogeological investigations and numerical simulation of groundwater flow in the karstic aquifer of northwestern Yucatan, Mexico. Coastal aquifer management: monitoring, modeling and case studies.
Meacham, S.S., 2012. Using Landsat 5 TM Data to Identify and Map Areas of Mangrove in Tulum, Quintana Roo, Mexico [Masters of Science: University of New Hampshire]. 105 p.
Metcalfe, S.E., O'Hara, S.L., Caballero, M., Davies, S.J., 2000. Records of Late Pleistocene–Holocene climatic change in Mexico—a review. Quat. Sci. Rev. 19 (7), 699–721.
Molina, C., Rubinoff, P., Carranza, J., 2001. Guidelines for Low Impact Tourism along the Coast of Quintana Roo. Mexico, Amigos de Sian Kal an, AC, Coastal Resources Center, Cancun, Quintana Roo, Mexico (accessed January 10th, 2003).
Neuman, B.R., Rahbek, M.L., 2007. Modeling the Groundwater Catchment of the Sian Ka'an Reserve. (*Quintana Roo*. Association for Mexican Cave Studies).
Orme, L.C., Reinhardt, L., Jones, R.T., Charman, D.J., Croudace, I., Dawson, A., Barkwith, A., 2016. Investigating the maximum resolution of μXRF core scanners: a 1800 year storminess reconstruction from the Outer Hebrides, Scotland, UK. The Holocene 26 (2), 235–247.
Parra, S.M., Valle-Levinson, A., Mariño-Tapia, I., Enriquez, C., Candela, J., Sheinbaum, J., 2016. Seasonal variability of saltwater intrusion at a point-source submarine groundwater discharge. Limnol. Oceanogr. 61 (4), 1245–1258.
Paytan, A., Shellenbarger, G.G., Street, J.H., Gonneea, M.E., Davis, K., Young, M.B., Moore, W.S., 2006. Submarine groundwater discharge: an important source of new inorganic nitrogen to coral reef ecosystems. Limnol. Oceanogr. 51 (1), 343–348.
Perry, E., Paytan, A., Pedersen, B., Velazquez-Oliman, G., 2009. Groundwater geochemistry of the Yucatan Peninsula, Mexico: constraints on stratigraphy and hydrogeology. J. Hydrol. 367 (1), 27–40.
Pohlman, J.W., Iliffe, T.M., Cifuentes, L.A., 1997. A stable isotope study of organic cycling and the ecology of an anchialine cave ecosystem. Mar. Ecol. Prog. Ser. 17–27.
Quintana Roo Speleological Survey, 2019. List of Long Underwater Caves in Quintana Roo. Tulum, Quintana Roo Speleological Survey, Mexico.
Revel, M., Bayon, G., Vigier, N., Bastian, L., Dufour, A., 2017. Abrupt response of chemical weathering to Late Quaternary hydroclimate changes in northeast Africa. Sci. Rep. 7 (1). https://doi.org/10.1038/srep442.
Rioual, P., Chu, G.Q., Li, D., Mingram, J., Han, J., Liu, J., 2009. Climate-induced shifts in planktonic diatoms in lake Sihailongwan (North-East China): a study of the sediment trap and palaeolimnological records. In: 11th International Paleolimnology Symposium, pp. 120.
Roy, P.D., Torrescano-Valle, N., del Socorro Escarraga-Paredes, D., Vela-Pelaez, A.A., Lozano-Santacruz, R., 2018. Comparison of elemental concentration in near-surface late Holocene sediments and rainfall regimes of the Yucatán Peninsula (Mexico): a preliminary study. BOLETIN GEOLOGICO Y MINERO 129 (4), 693–706.
Sánchez, M., Alcocer, J., Escobar, E., Lugo, A., 2002. Phytoplankton of cenotes and anchialine caves along a distance gradient from the northeastern coast of Quintana Roo, Yucatan Peninsula. Hydrobiologia 467 (1), 79–89.
Schmitter-Soto, J.J., Comín, F.A., Escobar-Briones, E., Herrera-Silveira, J., Alcocer, J., Suárez-Morales, E., Steinich, B., 2002. Hydrogeochemical and biological characteristics of cenotes in the Yucatan Peninsula (SE Mexico). Hydrobiologia 467 (1–3), 215–228.
Smart, P.L., Beddows, P.A., Coke, J., Doerr, S., Smith, S., Whitaker, F.F., 2006. Cave development on the Caribbean coast of the Yucatan Peninsula, Quintana Roo, Mexico. Geol. Soc. Am. Spec. Pap. 404, 105–128.
Smith, S.L., Whitaker, F.F., Parkes, R.J., Smart, P.L., Beddows, P.A., Bottrell, S.H., 2002. The geochemistry and geomicrobiology of saline groundwaters: Yucatan Peninsula, Mexico. Hydrogeology and Biology of Post-Paleozoic Carbonate Aquifers, Karst Waters Institute Special Publication 7, 135–137.
Sobel, A.H., Camargo, S.J., Hall, T.M., Lee, C.Y., Tippett, M.K., Wing, A.A., 2016. Human influence on tropical cyclone intensity. Science 353 (6296), 242–246.
Steinke, T.D., Holland, A.J., Singh, Y., 1993. Leaching losses during decomposition of mangrove leaf litter. S. Afr. J. Bot. 59 (1), 21–25.
Stoessell, R.K., Coke, J.G., 2006. An Explanation for the lack of a Dilute Freshwater Lens in Unconfined Tropical Coastal Aquifer. Yucatan Example: Gulf Coast Association of Geological Societies Transactions 56, 785–792.
Teranes, J.L., Bernasconi, S.M., 2000. The record of nitrate utilization and productivity limitation provided by δ15N values in lake organic matter—a study of sediment trap and core sediments from Baldeggersee, Switzerland. Limnol. Oceanogr. 45 (4), 801–813.
Thomson J, Croudace IW, Rothwell RG (2006) A geochemical application of the ITRAX scanner to a sediment core containing eastern Mediterranean sapropel units. In: Rothwell RG (ed) New Techniques in Sediment Core Analysis. Geol. Soc. Spec. Publ. 267:65–77. doi:https://doi.org/10.1144/GSL.SP.2006.267.01.05.
Torrescano-Valle, Islebe, 2012. Mangroves of Southeastern Mexico: Palaeoecology and Conservation.
Urban, N.R., Lu, X., Chai, Y., Apul, D.S., 2004. Sediment trap studies in Lake Superior: Insights into resuspension, cross-margin transport, and carbon cycling. J. Great Lakes Res. 30, 147–161.
Zhao, M.Y., Zheng, Y.F., 2015. The intensity of chemical weathering: Geochemical constraints from marine detrital sediments of Triassic age in South China. Chem. Geol. 391, 111–122.